Global constraints on muon-neutrino nonstandard interactions

F. J. Escrihuela,* M. Tórtola,† and J. W. F. Valle‡

Instituto de Física Corpuscular – C.S.I.C./Universitat de València, Campus de Paterna, Apt 22085, E–46071 València, Spain

O. G. Miranda§

Departamento de Física, Centro de Investigación y de Estudios Avanzados del IPN, Apdo. Postal 14-740 07000 Mexico, DF, Mexico

(Received 11 March 2011; published 4 May 2011)

The search for new interactions of neutrinos beyond those of the standard model may help to elucidate the mechanism responsible for neutrino masses. Here, we combine existing accelerator neutrino data with restrictions coming from a recent atmospheric neutrino data analysis in order to lift parameter degeneracies and improve limits on new interactions of muon neutrinos with quarks. In particular, we reconsider the results of the E-815 experiment at Fermilab (NuTeV) in view of a new evaluation of its systematic uncertainties. We find that, although constraints for muon neutrinos are better than those applicable to tau or electron neutrinos, they lie at the few $\times 10^{-2}$ level, not as strong as previously believed. We briefly discuss prospects for further improvement.

DOI: 10.1103/PhysRevD.83.093002 PACS numbers: 13.15.+g, 12.90.+b, 23.40.Bw

I. INTRODUCTION

The discovery of neutrino oscillations provides the only firm evidence for new physics we currently have [1], namely, neutrino mass. This constitutes the most important discovery in particle physics in the last quarter century, implying that the standard model, which correctly accounts for all other experimental data in particle physics, needs revision [2]. Precision is the keyword in neutrino physics today, including solar and atmospheric neutrino data analysis, as well as the determination of neutrino masses and mixing parameters at reactor and long-baseline accelerator experiments [3–5]. It is important not only to investigate the potential of current and upcoming long-baseline experiments to determine the neutrino oscillation parameters, but also to probe for the possible existence of nonstandard neutrino interactions, NSI for short. The latter are expected in most models of neutrino mass generation, such as seesaw-type schemes , and will play a crucial role since they will shed light on the scale characterizing this so-far elusive mass generation mechanism. The interest on probing for the existence of NSI has been growing over recent years, thanks also to the increasing precision of upcoming experiments [7,8] and to the fact that the current oscillation interpretation is not yet fully robust [9], so one needs to scrutinize the interplay between oscillations and NSI in future experiments [10–13].

A wide class of nonstandard neutrino interactions may be parametrized at low energies by the effective Lagrangian

$$-\mathcal{L}^{\rm eff}_{\rm NSI} = \sum_{\alpha\beta} \varepsilon^{fP}_{\alpha\beta} 2\sqrt{2} G_F (\bar{\nu}_\alpha \gamma_\rho L \nu_\beta)(\bar{f}\gamma^\rho P f), \quad (1)$$

where G_F is the Fermi constant and the parameters $\varepsilon^{fP}_{\alpha\beta}$ characterize the strength of the NSI. For simplicity, these are assumed to be real. The chiral projectors P denote $\{R, L = (1 \pm \gamma^5)/2\}$, while α and β label the three-neutrino flavors, e, μ and τ and f is a first generation charged SM fermion (e, u or d).

Collider experiments produce well-controlled and clean muon-neutrino beams, with just a small component of electron neutrinos, while tau neutrino beams are unavailable. As a result, one can expect that the muon-neutrino NSI parameters, $\varepsilon^{fP}_{\mu\beta}$ are better constrained in comparison with other neutrino flavors. This is indeed the case for the interaction with electrons [14,15]. However, for the interaction of neutrinos with quarks, although neutrino nucleon scattering has a very long history since CDHS [16] and CHARM [17], the accuracy of these early experiments was worse than that of the more recent NuTeV experiment, which has measured the $\nu_\mu N$ interaction with a very high accuracy [18], reporting a discrepancy with the standard model predictions. While this may be interpreted as a hint of new physics, indicating at face-value a potentially nonzero value for the NSI parameters $\varepsilon^{fP}_{\mu\alpha}$ [19], uncertainties coming from QCD corrections might have been underestimated [20].

Moreover, as expected, limits on muon-neutrino NSI coupling strengths [19] derived on the basis of 1-loop dressing of the neutrino effective four-fermion vertex can not be formulated rigorously. Indeed these are highly model dependent and, even when a full analysis is performed, including all the necessary diagrams required in order to obtain gauge-invariance, one does not strongly

*franesfe@alumni.uv.es
†mariam@ific.uv.es
‡valle@ific.uv.es, URL: http://astroparticles.es/
§Omar.Miranda@fis.cinvestav.mx

constrain the flavor-changing parameters $\varepsilon_{\mu\tau}^{qL,R}$ and $\varepsilon_{\mu e}^{qL,R}$ [21].

Recently, two new determinations of the standard model electroweak mixing parameter $\sin^2\theta_W$ from the NuTeV measurement have been presented [22,23]. Given that the most stringent model–independent bounds on $\varepsilon_{\mu\alpha}$ come from the NuTeV data, it is necessary to consider the effect of including these new corrections on the NuTeV results. Therefore, the main goal of this paper is to the review the current status of the constraints for the ν_μ nonstandard neutrino interactions in view of the larger uncertainties indicated by these recent papers. In so doing, we will not only take into account the new results mentioned above, but also combine the laboratory constraints with the restrictions inferred from the analysis of atmospheric neutrino data. In order to obtain these constraints, we adopt as a simplifying working hypothesis that all NSI parameters other than $\varepsilon_{\mu\alpha}^{qP}$ vanish. We will see that restricting ourselves to a two-generation NSI global analysis, we obtain relatively stringent constraints on the NSI interactions for muon neutrinos, at the few $\times\, 10^{-2}$ level, thanks largely to the interplay of atmospheric data.

The paper is planned as follows. In the next section, we will make a brief description of the neutrino nucleon scattering parameters that are relevant for our analysis. In Sec. III, we will discuss the NuTeV data and their implications for the NSI parameters, while in Sec. IV we discuss the previous experiments CHARM and CDHS. In Sec. V, we combine this information with constraints coming from the analysis of atmospheric neutrinos in order to obtain global constraints on the NSI parameters. Finally, in Sec. VI, we will give our conclusions and discuss the prospects for further improvement in the determination of NSI parameters.

II. θ_W MEASUREMENTS IN NEUTRINO–NUCLEON SCATTERING EXPERIMENTS

Neutrino scattering experiments provide one of the most precise probes of the weak neutral current, and have been often been used to measure the electroweak mixing angle $\sin^2\theta_W$. In particular, it has been shown that experiments with an isoscalar target are particularly convenient, since in this case the uncertainties due to unknown corrections to the QCD parton model cancel to a large extent [24]. For an isoscalar target of up and down-type quarks, the largest contributions to the neutral and charged current cross sections are related by isospin invariance; their ratio can be written as:

$$R^\nu = \frac{\sigma(\nu_\mu N \to \nu_\mu X)}{\sigma(\nu_\mu N \to \mu^- X)} = (g_\mu^L)^2 + r(g_\mu^R)^2 \tag{2}$$

$$R^{\bar\nu} = \frac{\sigma(\bar\nu_\mu N \to \bar\nu_\mu X)}{\sigma(\bar\nu_\mu N \to \mu^+ X)} = (g_\mu^L)^2 + \frac{1}{r}(g_\mu^R)^2 \tag{3}$$

where one introduces the ratio

$$r = \frac{\sigma(\bar\nu_\mu N \to \mu^+ X)}{\sigma(\nu_\mu N \to \mu^- X)} \tag{4}$$

and the coupling constants are defined as

$$(g_\mu^P)^2 = (g_\mu^{uP})^2 + (g_\mu^{dP})^2 \tag{5}$$

with $P = L, R$. In the presence of NSI of muon neutrinos with quarks, these coupling constants are replaced by:

$$(\tilde g_\mu^L)^2 = (g_\mu^{uL} + \varepsilon_{\mu\mu}^{uL})^2 + (g_\mu^{dL} + \varepsilon_{\mu\mu}^{dL})^2 + \sum_{\alpha\neq\mu}|\varepsilon_{\mu\alpha}^{uL}|^2 + \sum_{\alpha\neq\mu}|\varepsilon_{\mu\alpha}^{dL}|^2 \tag{6}$$

$$(\tilde g_\mu^R)^2 = (g_\mu^{uR} + \varepsilon_{\mu\mu}^{uR})^2 + (g_\mu^{dR} + \varepsilon_{\mu\mu}^{dR})^2 + \sum_{\alpha\neq\mu}|\varepsilon_{\mu\alpha}^{uR}|^2 + \sum_{\alpha\neq\mu}|\varepsilon_{\mu\alpha}^{dR}|^2 \tag{7}$$

The quantities R^ν and $R^{\bar\nu}$ have been measured in the past at the CDHS [16] and CHARM experiments [17]. Another well-known observable for the study of deep inelastic neutrino scattering on an isoscalar target is the Paschos-Wolfenstein (PW) ratio, defined as [25]

$$R_{\rm PW} = \frac{\sigma(\nu_\mu N \to \nu_\mu X) - \sigma(\bar\nu_\mu N \to \bar\nu_\mu X)}{\sigma(\nu_\mu N \to \mu^- X) - \sigma(\bar\nu_\mu N \to \mu^+ X)} = \frac{R^\nu - rR^{\bar\nu}}{1-r} = (g_\mu^L)^2 - (g_\mu^R)^2. \tag{8}$$

This ratio is particularly useful because it depends very weakly on the hadronic structure of the nucleus target, and it is largely insensitive to the uncertainties resulting from charm production as well as charm and strange sea distributions. However, the simultaneous measurement of neutral current cross sections for neutrinos and antineutrinos requires the use of separate neutrino and antineutrino beams. The NuTeV Collaboration makes use of this observable in order to measure the electroweak mixing angle. Actually, they measure experimentally the ratios R_ν and $R_{\bar\nu}$, shown in Eqs. (2) and (3), which later transform in the Paschos-Wolfenstein ratio R_{PW} through their fit procedure.

III. CONSTRAINTS FROM NUTEV DATA

The NuTeV collaboration used high statistics neutrino and antineutrino beams to measure their neutral and charged current cross sections on an iron target. Using a statistical separation of the NC and CC event candidates, based on the length of each event in the detector, NuTeV reported experimental values for R_ν and $R_{\bar\nu}$, as mentioned in the previous section. A numerical fit of these results provides a measurement of the left and right-handed neutral couplings to the light quarks [18]:

$$(g_\mu^L)^2 = 0.30005 \pm 0.00137 \tag{9}$$

$$(g_\mu^R)^2 = 0.03076 \pm 0.00110. \tag{10}$$

Notice the discrepancy with respect to the standard model expectations [1]:

$$\begin{aligned}(g_\mu^L)^2_{\rm SM} &= 0.30399 \pm 0.00017\\ (g_\mu^R)^2_{\rm SM} &= 0.03001 \pm 0.00002,\end{aligned} \tag{11}$$

due to the NuTeV preference for a lower effective left-handed coupling, almost 3σ away from the SM expectation. Similarly, a value for the electroweak mixing angle in the on-shell scheme was obtained from a numerical fit:

$$\sin^2\theta_W = 0.22773 \pm 0.00135^{\rm stat} \pm 0.00093^{\rm syst} \tag{12}$$

which is 3σ away from the value determined in global precision electroweak fits [1]:

$$\sin^2\theta_W = 0.22292 \pm 0.00082. \tag{13}$$

Ascribing the discrepancy between the NuTeV result for the left coupling $(g_\mu^L)^2$ and its prediction within the standard model to the existence of a nonzero NSI-operator, the authors in Ref. [19] obtained a positive hint for nonzero values of the left flavor-conserving NSI couplings $\varepsilon_{\mu\mu}^{dL}$ and $\varepsilon_{\mu\mu}^{uL}$. On the other hand, for the case of flavor-changing NSI parameters, they obtained limits on the NSI $|\varepsilon_{\mu\tau}^{qL;R}|$ couplings.

However, several corrections and theoretical uncertainties coming, for instance, from nuclear effects and next-to-leading-order corrections were neglected in the original NuTeV Collaboration analysis. Although the presence of NSI could explain the discrepancy of the NuTeV results with the SM, before claiming that they provide a hint of new physics one needs make sure that all uncertainties are carefully taken into account. As a matter of fact, several attempts have been made to interpret the NuTeV results just in terms of conventional physics; see, for example, Refs. [20,26].

Here, we reanalyze the impact of taking into account carefully the uncertainties in deriving restrictions on physics beyond the SM as parametrized by the NSI Lagrangian in Eq. (1). In particular, we will focus on the two most recent reanalyses of the NuTeV data given in Refs. [22,23] in order to obtain constraints on neutrino NSI coupling strengths.

The NNPDF Collaboration reports more precise estimates of the strange and antistrange parton distribution functions, leading to a new value for the electroweak mixing angle [22]:

$$\sin^2\theta_W = 0.2263 \pm 0.0014^{\rm stat} \pm 0.0009^{\rm sys} \pm 0.0107^{\rm PDFs}. \tag{14}$$

On the other hand, the analysis in Ref. [23] takes into account three different corrections coming from nuclear effects, due to the excess of neutrons in iron, charge symmetry violation arising from up and down quark mass differences, and strange quarks. With all these corrections included, the following value for the electroweak mixing angle is extracted:

$$\sin^2\theta_W = 0.2232 \pm 0.0013^{\rm stat} \pm 0.0024^{\rm sys}. \tag{15}$$

One can see from Eqs. (14) and (15) that the two recalculated estimates for the electroweak mixing angle, with larger uncertainties, are consistent with the SM prediction, as seen in Fig. 1. In order to determine the resulting restrictions set by NuTeV data on the strength of NSI couplings, in view of the corrections discussed above [22,23], we adopt the Paschos-Wolfenstein ratio $R_{\rm PW}$. We perform a χ^2 analysis using the Paschos-Wolfenstein ratio derived from each reanalysis of NuTeV data, and we compare these results with the Ssandard model prediction for R_{PW}. As a result of this simple statistical analysis, and allowing for one nonzero NSI coupling at a time, we obtain the following constraints at 90% C.L. :

$$\begin{aligned}&-0.017 < \varepsilon_{\mu\mu}^{dL} < 0.025 \;\;\&\;\; 0.84 < \varepsilon_{\mu\mu}^{dL} < 0.88,\\ &-0.24 < \varepsilon_{\mu\mu}^{dR} < 0.088,\end{aligned} \tag{16}$$

$$\begin{aligned}&-0.72 < \varepsilon_{\mu\mu}^{uL} < -0.67 \;\;\&\;\; -0.031 < \varepsilon_{\mu\mu}^{uL} < 0.020,\\ &-0.058 < \varepsilon_{\mu\mu}^{uR} < 0.063 \;\;\&\;\; 0.24 < \varepsilon_{\mu\mu}^{uR} < 0.36,\end{aligned} \tag{17}$$

when using the results in NNPDF, and

$$\begin{aligned}&-0.005 < \varepsilon_{\mu\mu}^{dL} < 0.005 \quad \& \quad 0.86 < \varepsilon_{\mu\mu}^{dL} < 0.87,\\ &-0.17 < \varepsilon_{\mu\mu}^{dR} < -0.11 \quad \& \quad -0.042 < \varepsilon_{\mu\mu}^{dR} < 0.025,\end{aligned} \tag{18}$$

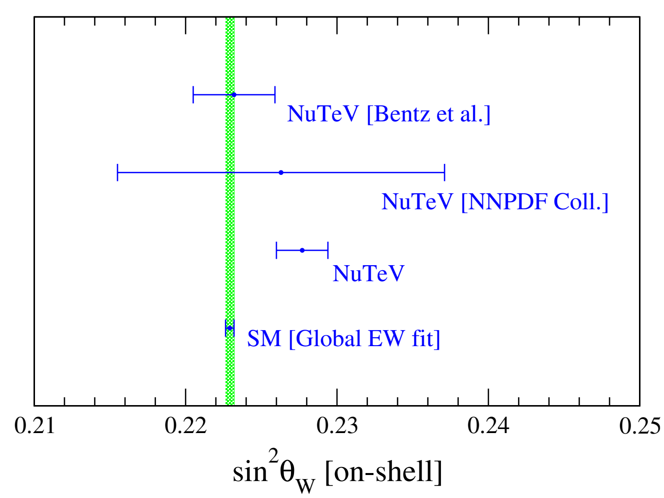

FIG. 1 (color online). Current status of $\sin^2\theta_W$ determinations from Refs. [1,18,22,23].

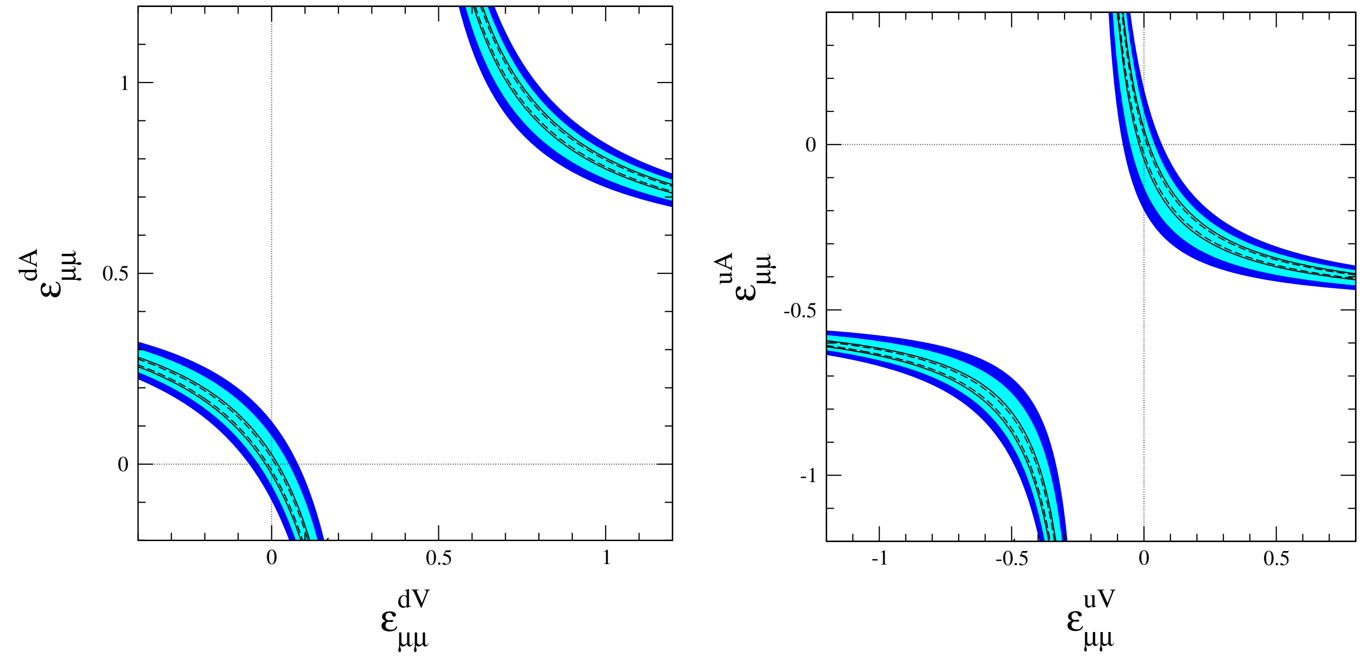

FIG. 2 (color online). Allowed regions at 90% C.L. and 3σ for the vectorial and axial NSI couplings of neutrinos with down (left panel) and up-type (right panel) quarks. Shaded regions are obtained using NNPDF corrections [22], while empty lines correspond to Bentz *et al.* [23].

$$-0.71 < \varepsilon^{uL}_{\mu\mu} < 0.70 \;\; \& \;\; -0.006 < \varepsilon^{uL}_{\mu\mu} < 0.006,$$
$$-0.014 < \varepsilon^{uR}_{\mu\mu} < 0.016 \;\; \& \;\; 0.28 < \varepsilon^{uR}_{\mu\mu} < 0.31 \qquad (19)$$

for the Bentz *et al.* case. For both analyses we observe two allowed regions for most of the NSI couplings, reflecting the degeneracy seen in Fig. 2.

Allowing now for the simultaneous presence of left and right–handed NSI neutrino couplings, we obtain the results given in Fig. 2. For convenience, we present the constraints in terms of the vector and axial couplings instead of using the L, R basis. This makes it easier to proceed when combining with the atmospheric data (see below). The left panel holds for the case of a down-type quark, while the right one holds for an up-type quark. Here, as well as in Sec. V, the allowed regions for the neutrino NSI couplings have been obtained separately for down and up-type quarks, assuming the presence of NSI with only one type of quark in each case. One can see that, in both cases, there is a two-fold degeneracy in the values of the NSI parameters, which is easily understood from Eq. (8).[1] On the other hand, for the case of flavor-changing NSI, our analysis gives the allowed region shown in Fig. 3. In this case, the allowed regions for the two chiral components of the flavor-changing NSI couplings of u- and d-type quarks

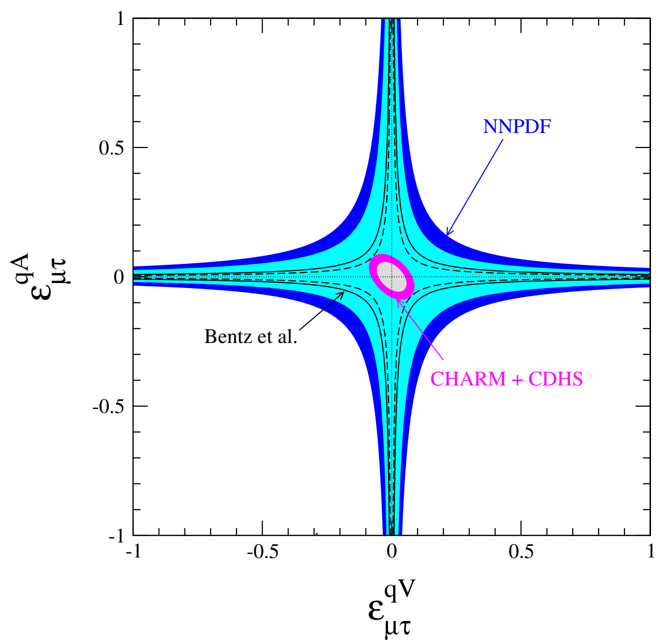

FIG. 3 (color online). Same as Fig. 2 for the flavor-changing couplings of up- and down-type quarks with neutrinos. Colored regions are obtained using NNPDF corrections [22], while empty lines correspond to the Bentz *et al.* reanalysis [23]. The small region in the shaded ellipse results from the analysis of CHARM and CDHS results, see discussion in Secs. IV and VI.

[1] Note that in terms of the NSI couplings $\varepsilon^{qL}_{\mu\mu}$, $\varepsilon^{qR}_{\mu\mu}$, this equation represents a hyperbola centered at $(\varepsilon^{qL}_{\mu\mu}, \varepsilon^{qR}_{\mu\mu}) = (-g^{qL}_{\mu}, -g^{qR}_{\mu})$. After the change of variables to $(\varepsilon^{qV}_{\mu\mu}, \varepsilon^{qA}_{\mu\mu})$, the hyperbola is rotated to the one shown in Fig. 2.

TABLE I. Ratios of neutral to charged currents measured by CHARM and CDHS compared with the SM prediction.

Experiment	Observable	measurement	SM prediction
CDHS [16]	R^{ν}	0.3072 ± 0.0033	0.3208
	$R^{\bar{\nu}}$	0.382 ± 0.016	0.381
	r	0.393 ± 0.014	
CHARM [17]	R^{ν}	0.3093 ± 0.0031	0.3226
	$R^{\bar{\nu}}$	0.390 ± 0.014	0.371
	r	0.456 ± 0.011	

are the same, hence we show our results in only one plot. Note that here the allowed region is a hyperbola centered at the origin $(\varepsilon_{\mu\tau}^{qV}, \varepsilon_{\mu\tau}^{qA}) = (0, 0)$, displaying a remnant of the two-fold degeneracy seen for the flavor-conserving case. In agreement with Eqs. (6)–(8), our analysis constrains the product $\varepsilon_{\mu\tau}^{qV} \cdot \varepsilon_{\mu\tau}^{qA}$, and therefore, one coupling could be of order one, provided that the other one is small enough. As before, the different widths for the allowed regions for each reanalysis of NuTeV data reflect the experimental errors calculated in each case.

IV. CONSTRAINTS FROM CHARM AND CDHS

Both the CHARM and CDHS experiments have measured semileptonic neutrino scattering cross sections. Although these early experiments have a lower sensitivity than that reached at the NuTeV experiment, their data are still useful in our global analysis. While these two experiments can not compete with the NuTeV sensitivity in constraining the strength of nonuniversal NSI couplings, they play an important role in restricting that of the flavor-changing NSI[2] and for this reason we consider them in our analysis. The measurements of these experiments are summarized in Table I. Using the information given in this table, we perform a χ^2 analysis, including the correlation between the neutrino and antineutrino ratios of neutral to charged currents given by the parameter r. Our χ^2 function in this case is given by

$$\chi^2 = \sum_i \chi_i^2 = \sum_{j,k} (R_i^j - R_{i,\mathrm{NSI}}^j)(\sigma^2)_{jk}^{-1}(R_i^k - R_{i,\mathrm{NSI}}^k) \qquad (20)$$

where i runs for either CHARM or CDHS and j, k stands for R^{ν} and $R^{\bar{\nu}}$. The results of our computation are shown in Fig. 3. Although the inclusion of these data strongly constrains the axial flavor-changing NSI parameters, the restriction follows from a discrepancy between the experimental and the theoretical value of R^{ν}, as can be seen from Table I. As already mentioned, this results in a very a poor fit; hence, we warn that constraints obtained for this case should be considered as less robust than those obtained for nonuniversal NSI discussed above. For the sake of completeness, however, and in analogy with Eqs. (16)–(19), we quote the constraints that would be obtained at 90% C.L. by combining CHARM/CDHS with the reanalysis of NuTeV data performed by the NNPDF Collaboration (or Bentz *et al.*):

$$-0.023(-0.023) < \varepsilon_{\mu\tau}^{qL} < 0.023(0.023),$$
$$-0.039(-0.036) < \varepsilon_{\mu\tau}^{qR} < 0.039(0.036). \qquad (21)$$

V. COMBINING WITH ATMOSPHERIC DATA

Atmospheric neutrino data are well described by the standard mechanism of neutrino oscillations [4,5]. As a result, if neutrino NSI with matter exist, they must at best play a subleading role in the description of atmospheric neutrino data. We now discuss atmospheric neutrino propagation in the presence of non-standard neutrino-matter interactions, containing both flavor-changing and flavor-diagonal components [27–29]. In the context of such hybrid scheme, the presence of neutrino NSI would affect atmospheric neutrino propagation in matter introducing an extra term in the evolution Hamiltonian. In the simple two-neutrino description, the NSI contribution to the Hamiltonian will be given by

$$H_{\mathrm{NSI}} = \sqrt{2} G_F N_q \begin{pmatrix} \varepsilon_{\mu\mu}^{qV} & \varepsilon_{\mu\tau}^{qV} \\ \varepsilon_{\mu\tau}^{qV} & \varepsilon_{\tau\tau}^{qV} \end{pmatrix} \qquad (22)$$

with $q = u, d$ and $\varepsilon_{\alpha\beta}^{qV} = \varepsilon_{\alpha\beta}^{qL} + \varepsilon_{\alpha\beta}^{qR}$, where one notes that neutrino propagation is only sensitive to the vectorial NSI couplings. This provides important information complementary to that coming from the accelerator experiments, see Eqs. (6) and (7).

The Super-Kamiokande neutrino data have been analyzed under this assumption in Refs. [27–29]. Up to now, no evidence of NSI has been found in the atmospheric data sample and, as a result, one gets upper bounds on the magnitude of the NSI coupling strengths. Here we will include in our analysis the most recent published results using the full atmospheric SK-I and SK-II data sample [29] which leads to the following bounds:

$$0.007 < \varepsilon_{\mu\tau}^{dV} < 0.007 \qquad (23)$$

[2]The only caveat, however, is the bad quality of the resulting fit, given that these old experiments are not in good agreement with the SM, and that the addition of NSI only makes it worse.

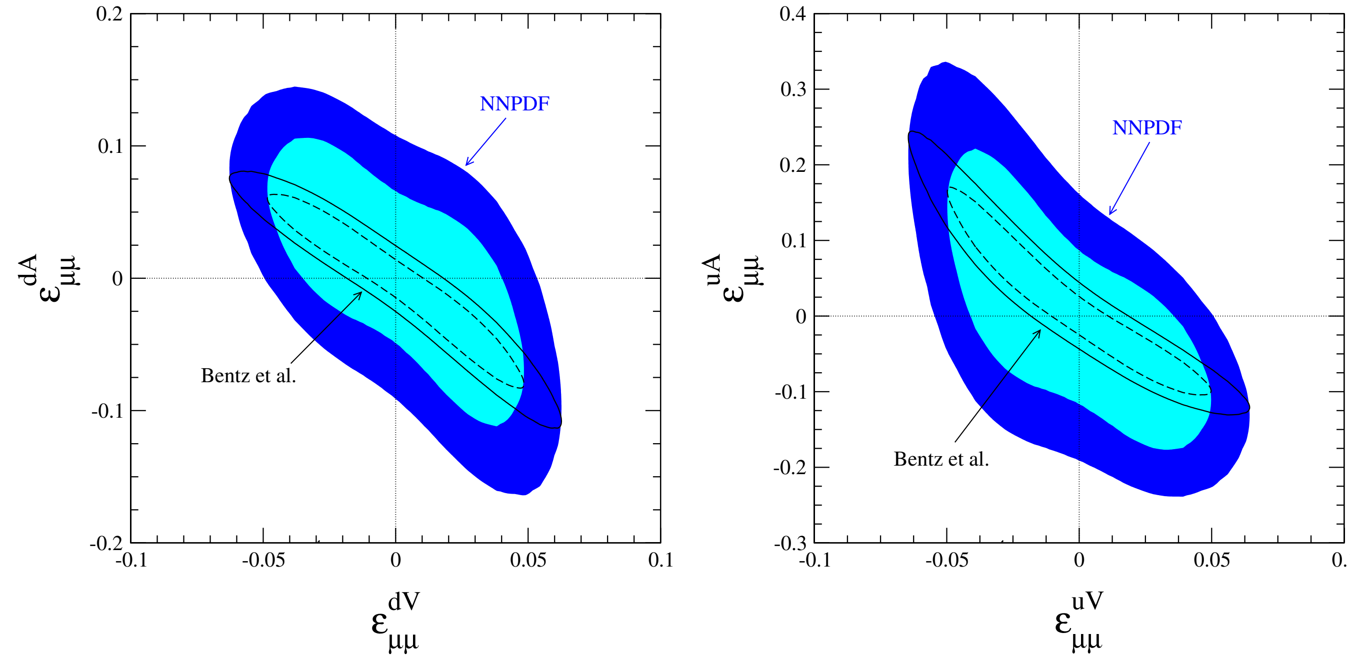

FIG. 4 (color online). Allowed regions at 90% C.L. and 3σ for flavor-diagonal NSI couplings of down- (left panel) and up-type quarks (right panel) with neutrinos obtained by combining accelerator data with results from the atmospheric data analysis. We use the same conventions as in Fig. 2.

$$|\varepsilon^{dV}_{\tau\tau} - \varepsilon^{dV}_{\mu\mu}| < 0.042, \tag{24}$$

at 90% C.L. (1 d.o.f.). These limits have been obtained for the case of neutrino NSI with down-type quarks. Taking into account the chemical composition of the Earth in the Preliminary Reference Earth Model (PREM) model [30], we can rewrite the bounds on Eq. (24) in terms of the neutrino NSI couplings with up-type quarks to a good approximation. According to Ref. [31], the ratio between the density of down and up quarks N_d/N_u takes a value of 1.009 (1.047) in the mantle (core) of the Earth. Using the average value: $N_d/N_u = 1.028$, one obtains the following 90% C.L. bounds on the neutrino—up quark NSI couplings:

$$0.007 < \varepsilon^{uV}_{\mu\tau} < 0.007 \tag{25}$$

$$|\varepsilon^{uV}_{\tau\tau} - \varepsilon^{uV}_{\mu\mu}| < 0.043. \tag{26}$$

We now go one step further combining also these results with those of the previous accelerator analysis. The constraints derived from such a combined analysis are shown in Figs. 4 and 5 for the case of flavor-diagonal and flavor-changing NSI, respectively. As before, for the nonuniversal NSI couplings we consider NuTeV, while for the flavor-changing couplings we also include the results of CHARM and CDHS. As seen in the previous section, for the case of flavor-changing NSI, the NuTeV accelerator results and atmospheric neutrino bounds are nearly the same for up- or down-type quarks, and therefore we only present the plot for down-type quarks. One sees that the atmospheric neutrino data provide quite a useful tool to constrain the vector NSI coupling parameter, allowing to remove the degeneracy discussed before.

Once we make the projection of the two parameter analysis into one parameter, we obtain the following

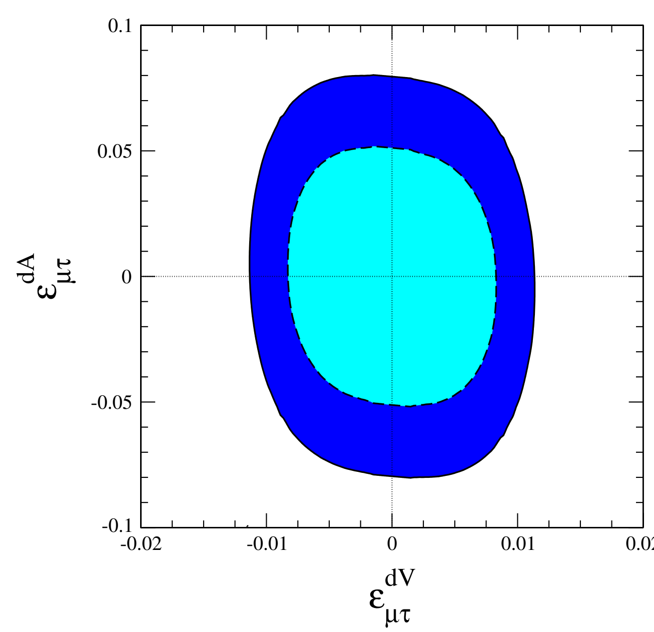

FIG. 5 (color online). Same as Fig. 4 for the flavor-changing NSI couplings with down-type quarks, with nearly the same results for up-type quarks. The two reanalyses on NuTeV data considered here lead to the same results, since the analysis is dominated by atmospheric and CHARM + CDHS data.

TABLE II. Allowed values for NSI parameters from a global analysis of NuTeV data using NNPDF and Bentz *et al.* corrections, combined with atmospheric data. The top of the table corresponds to nonuniversal (NU) NSI parameters and the bottom to flavor-changing (FC) NSI. In the latter case, CDHS and CHARM data are also included.

Global with NuTeV reanalysis	NSI with down	NSI with up
	NU	NU
NNPDF [22]	$-0.042 < \varepsilon_{\mu\mu}^{dV} < 0.042$	$-0.044 < \varepsilon_{\mu\mu}^{uV} < -0.044$
	$-0.091 < \varepsilon_{\mu\mu}^{dA} < 0.091$	$-0.15 < \varepsilon_{\mu\mu}^{uA} < 0.18$
Bentz *et al.* [23]	$-0.042 < \varepsilon_{\mu\mu}^{dV} < 0.042$	$-0.044 < \varepsilon_{\mu\mu}^{uV} < -0.044$
	$-0.072 < \varepsilon_{\mu\mu}^{dA} < 0.057$	$-0.094 < \varepsilon_{\mu\mu}^{uA} < 0.14$
	FC	FC
NNPDF/Bentz *et al.*	$-0.007 < \varepsilon_{\mu\tau}^{dV} < 0.007$	$-0.007 < \varepsilon_{\mu\tau}^{uV} < 0.007$
	$-0.039 < \varepsilon_{\mu\tau}^{dA} < 0.039$	$-0.039 < \varepsilon_{\mu\tau}^{uA} < 0.039$

constraints at 90% C.L. when considering the reanalysis of the NuTeV anomaly reported by Refs. [22] ([23]):

$$-0.042(-0.042) < \varepsilon_{\mu\mu}^{dV} < 0.042(0.042),$$
$$-0.091(-0.072) < \varepsilon_{\mu\mu}^{dA} < 0.091(0.057) \tag{27}$$

$$-0.044(-0.044) < \varepsilon_{\mu\mu}^{uV} < -0.044(0.044),$$
$$-0.15(-0.094) < \varepsilon_{\mu\mu}^{uA} < 0.18(0.14). \tag{28}$$

For the case of the flavor-changing parameters, the results are nearly the same for the two different reanalysis of NuTeV data, since the determination of the vectorial couplings $\varepsilon_{\mu\tau}^{qV}$ are dominated by the atmospheric neutrino analysis, while the axial couplings $\varepsilon_{\mu\tau}^{qA}$ are mainly given by the accelerator experiments CHARM and CDHS. One finds,

$$-0.007 < \varepsilon_{\mu\tau}^{dV} < 0.007, \quad -0.039 < \varepsilon_{\mu\tau}^{dA} < 0.039 \tag{29}$$

$$-0.007 < \varepsilon_{\mu\tau}^{uV} < 0.007, \quad -0.039 < \varepsilon_{\mu\tau}^{uA} < 0.039. \tag{30}$$

A more complete full-fledged three-neutrino global analysis in the context of neutrino oscillations plus nonstandard interactions will introduce three additional NSI couplings, namely ε_{ee}, $\varepsilon_{e\mu}$, and $\varepsilon_{e\tau}$ and, as a result, the bounds would be correspondingly weaker.

VI. DISCUSSION AND FUTURE PROSPECTS

We have re-analyzed the constraints on novel nonstandard neutrino interactions of muon neutrinos with quarks, which follow from current accelerator experiments. In particular, we have reconsidered the results of the NuTeV experiment in view of a new evaluation of the NuTeV systematic uncertainties. We have combined the restrictions following from accelerator data with those coming from recent atmospheric data analysis, which plays a crucial role in removing degeneracies. We have found that, although constraints for muon neutrinos are better than those applicable to tau or electron neutrinos, they are not as strong as previously believed. While previous authors report bounds of the order of few $\times 10^{-3}$, we find that, taking into account the current estimates of the NuTeV uncertainties, constraints are now of the order of few $\times 10^{-2}$. Our results are summarized in Table II. Even weaker constraints would hold in a generalized three-generation framework. Although muon-neutrino NSI couplings are often neglected [32], one should keep in mind the weakness of the existing limits.

Note that these results will not be improved by the inclusion of data from the long-baseline experiment MINOS [33], given its poor sensitivity to matter effects when compared with that of atmospheric data, at least in a two-neutrino analysis. As a result, MINOS will not significantly restrict the neutral current NSI couplings discussed here, and the same is expected for OPERA [34]. However, future "clean" measurements of the oscillation parameters combined with the NSI-contaminated parameters determined by atmospheric experiments would be helpful. Certainly, it would also help considerably to have a very long-baseline setup as envisaged in the Long-Baseline Neutrino Experiment (LBNE) project currently proposed, capable of probing Earth matter effects with enhanced sensitivity [35].

Last, but not least, we note that a new high statistics neutrino scattering experiment, NuSOnG has been proposed [36], with the same goals as NuTeV. One of its main tasks would be to probe new physics in the neutrino couplings. Expectations are that NuSOnG would improve the NuTeV sensitivities on muon-neutrino quark scattering by a factor 2 at least, which would translate into a similar improvement on the NSI sensitivities with respect to those obtained from NuTeV.

ACKNOWLEDGMENTS

We would like to thank I. Cloet for useful comments about his work in Ref. [23]. Work supported by MICINN grants FPA2008-00319/FPA, CSD2009-00064, by PROMETEO/2009/091, by CONACyT and by EU network PITN-GA-2009-237920. M. T. acknowledges financial support from CSIC under the JAE-Doc programme.

[1] K. Nakamura *et al.* (Particle Data Group), J. Phys. G **37**, 075021 (2010).
[2] H. Nunokawa, S. J. Parke, and J. W. F. Valle, Prog. Part. Nucl. Phys. **60**, 338 (2008).
[3] T. Schwetz, M. Tortola, and J. W. F. Valle, arXiv:1103.0734.
[4] T. Schwetz, M. Tortola, and J. W. F. Valle, New J. Phys. **10**, 113011 (2008).
[5] M. Maltoni, T. Schwetz, M. A. Tortola, and J. W. F. Valle, New J. Phys. **6**, 122 (2004).
[6] J. Schechter and J. W. F. Valle, Phys. Rev. D **22**, 2227 (1980); **25**, 774 (1982).
[7] A. Bandyopadhyay *et al.* (ISS Physics Working Group), Rep. Prog. Phys. **72**, 106201 (2009).
[8] P. Huber, M. Lindner, T. Schwetz, and W. Winter, J. High Energy Phys. 11 (2009) 044.
[9] O. G. Miranda, M. A. Tortola, and J. W. F. Valle, J. High Energy Phys. 10 (2006) 008.
[10] P. Huber, T. Schwetz, and J. W. F. Valle, Phys. Rev. Lett. **88**, 101804 (2002).
[11] P. Huber, T. Schwetz, and J. W. F. Valle, Phys. Rev. D **66**, 013006 (2002).
[12] P. Huber and J. W. F. Valle, Phys. Lett. B **523**, 151 (2001).
[13] P. Huber and J. Kopp, J. High Energy Phys. 03 (2011) 013.
[14] J. Barranco *et al.*, Phys. Rev. D **77**, 093014 (2008).
[15] A. Bolanos *et al.*, Phys. Rev. D **79**, 113012 (2009).
[16] A. Blondel *et al.*, Z. Phys. C **45**, 361 (1990).
[17] J. V. Allaby *et al.* (CHARM collaboration), Z. Phys. C **36**, 611 (1987).
[18] G. P. Zeller *et al.* (NuTeV collaboration), Phys. Rev. Lett. **88**, 091802 (2002).
[19] S. Davidson, C. Pena-Garay, N. Rius, and A. Santamaria, J. High Energy Phys. 03 (2003) 011.
[20] S. Davidson, S. Forte, P. Gambino, N. Rius, and A. Strumia, J. High Energy Phys. 02 (2002) 037.
[21] C. Biggio, M. Blennow, and E. Fernandez-Martinez, J. High Energy Phys. 03 (2009) 139.
[22] R. D. Ball *et al.* (The NNPDF collaboration), Nucl. Phys. **B823**, 195 (2009).
[23] W. Bentz, I. C. Cloet, J. T. Londergan, and A. W. Thomas, Phys. Lett. B **693**, 462 (2010).
[24] C. H. Llewellyn Smith, Nucl. Phys. **B228**, 205 (1983).
[25] E. A. Paschos and L. Wolfenstein, Phys. Rev. D **7**, 91 (1973).
[26] K. S. McFarland and S. O. Moch, arXiv:hep-ph/0306052.
[27] N. Fornengo *et al.*, Phys. Rev. D **65**, 013010 (2001).
[28] M. C. Gonzalez-Garcia and M. Maltoni, Phys. Rep. **460**, 1 (2008).
[29] G. Mitsuka (Super-Kamiokande collaboration), Proc. Sci., NUFACT08 (2008) 059.
[30] A. M. Dziewonski and D. L. Anderson, Phys. Earth Planet. Inter. **25**, 297 (1981).
[31] E. Lisi and D. Montanino, Phys. Rev. D **56**, 1792 (1997).
[32] F. J. Escrihuela, O. G. Miranda, M. A. Tortola, and J. W. F. Valle, Phys. Rev. D **80**, 105009 (2009).
[33] D. G. Michael *et al.* (MINOS Collaboration), Phys. Rev. Lett. **97**, 191801 (2006).
[34] M. Blennow, D. Meloni, T. Ohlsson, F. Terranova, and M. Westerberg, Eur. Phys. J. C **56**, 529 (2008).
[35] Milind Diwan (private communication). See also: http://lbne.fnal.gov/.
[36] T. Adams *et al.* (NuSOnG collaboration), Int. J. Mod. Phys. A **24**, 671 (2009).